TESTING FUNDAMENTAL PHYSICS WITH CLOCKS IN SPACE: THE ACES MISSION

L. Cacciapuoti[a], P. Laurent[b], D. Massonnet[c], C. Salomon[d]
[a] *European Space Agency, Keplerlaan 1, 2200 AG Noordwijk ZH - The Netherlands*
Luigi.Cacciapuoti@esa.int
[b] *SYRTE, CNRS UMR 8630, Observatoire de Paris, LNE, UPMC, 61 Av. de l'Observatoire, 75014 Paris - France*
[c] *CNES, Centre Spatial de Toulouse, 18 Avenue Edouard Belin, 31401 Toulouse - France*
[d] *Laboratoire Kastler Brossel, ENS-PSL Research University, CNRS, UPMC, Collège de France, 24 rue Lhomond, 75005, Paris - France*

Atomic clocks and high-performance links are used to measure time and frequency to accuracy levels never reached before. When operated in a space-based laboratory, the large variations of the gravitational potential, the large velocities and velocity variations, as well as the worldwide access to ground clocks become key ingredients to measure tiny deformations in space-time that might bring the signature of new physics and new fundamental constituents. From the International Space Station, the ACES payload will distribute a clock signal with fractional frequency stability and accuracy of $1 \cdot 10^{-16}$. The comparison of distant clocks via ACES will be used to test Einstein's theory of general relativity. The ACES mission elements are now close to flight maturity. The flight model of the cold cesium clock PHARAO has been tested and delivered for integration in the ACES payload. Tests on the active hydrogen maser SHM and the microwave link MWL have been completed and manufacturing of the flight models is ongoing. The time transfer optical link ELT is also well advanced. This paper presents the progress of the ACES mission elements.

1 ACES Mission Elements

Clocks and interferometers based on samples of ultracold atoms are today state-of-the-art instruments for the measurement of time and frequency, accelerations, rotations, and faint forces. The sensitivity of these devices increases as the interaction time of the atomic sample with the probing electromagnetic field increases. In many of these instruments, e.g. fountain clocks and atom interferometers, atoms interrogation takes place during the free evolution of the sample in the gravity field. The most severe constraint to their performance is therefore imposed by gravity, which limits the maximum free fall time of the atoms in the limited volume of the apparatus. Operating these instruments in space becomes very attractive for the long interaction times that can be achieved in a freely falling laboratory.

Proposed to the European Space Agency in 1997, the *Atomic Clock Ensemble in Space* (ACES) mission relies on PHARAO, a clock based on laser-cooled caesium atoms, to generate a high stability and accuracy time reference in space[1,2]. The free fall conditions are crucial for PHARAO to reach or even surpass the performance of the best atomic fountain clocks on ground, while keeping a very compact volume, small mass, and power consumption. Installed onboard the International Space Station (ISS), at the external payload facility of the Columbus module, the ACES payload distributes its time scale to ground clocks by using two independent time & frequency transfer links, a link operating in the microwave domain (MWL) and the ELT (European Laser Timing) optical link. On the ground, a network of MWL ground terminal and satellite laser ranging stations

provides the physical interface between the ACES clock ensemble and atomic clocks on ground.

The ACES payload is shown in Figure 1. It has a volume of about $1\,m^3$, for a mass of 230 kg and a power consumption of 450 W. The main onboard instruments are the cesium clock PHARAO and the active hydrogen maser SHM. The PHARAO clock reaches a fractional frequency stability of $1 \cdot 10^{13}/\sqrt{\tau}$, where τ is the integration time expressed in seconds, and an accuracy of a few parts in 10^{16}. SHM is the ACES flywheel oscillator, also providing the frequency reference needed for the onboard characterization of the PHARAO clock accuracy. PHARAO and SHM 100 MHz signals are compared in the phase comparator FCDP, which also distributes the ACES frequency reference to MWL electronics. MWL is the ACES metrology link: coherently with the ACES clock signal, it generates the ACES time scale and compares it with the time scales locally generated by atomic clocks on the ground; furthermore, it stamps the arrival of the electrical pulses generated by the ELT detector in the onboard time. Finally, a GNSS receiver, tracking GPS, GALILEO and GLONASS signals, provides precise orbit data of the ACES clocks.

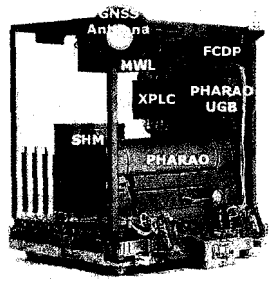

Figure 1 – The ACES payload has a volume of $1\,m^3$, for a mass of 230 kg, and a power consumption of 450 W.

Figure 2 shows the ACES network of MWL ground terminals. Seven fixed units will be deployed around the world, at the best institutes for time & frequency metrology: two in the US, JPL (Pasadena) and NIST (Boulder), three in Europe, at SYRTE (Paris, FR), PTB (Braunschweig, DE), and NPL (Teddington, UK), one in Japan, NICT (Tokyo), and one in the southern hemisphere, at UWA (Perth, AU). Furthermore, one transportable MWL station will be located in Europe and shared by other institutes, including the Wettzell geodetic observatory (Wettzell, DE), INRIM (Torino, IT), and METAS (Bern, CH); a second transportable station will be dedicated to the calibration of MWL fixed terminals for time transfer experiments and for comparisons with the laser link ELT. As shown in Figure 2, space-to-ground comparisons will occur over 4 continents, at the same time enabling ground-to-ground comparisons over intercontinental distances by using ACES as a relay satellite.

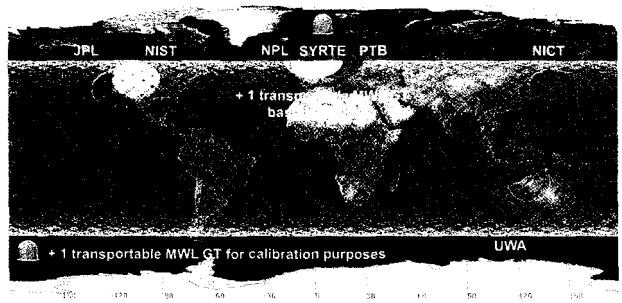

Figure 2 – The ACES network of MWL ground terminals and typical ground tracks of the ISS orbit.

Combined with the growing network of regional links using compensated optical fibers, which have already demonstrated frequency comparison capability at $1 \cdot 10^{-19}$ resolution, clock comparisons at the level of $1 \cdot 10^{-17}$ or better will soon be available with ACES on a worldwide scale. Such performance represents one to two orders of magnitude improvement over the currently used TW-STFT and GPS time transfer systems. Several institutes, such as PTB and SYRTE, are already interconnected by a fiber link and additional links will be operational by the time of the ACES mission. Furthermore, the fiber links between NIST and JILA (Boulder, US) as well as between NICT, NMIJ (Tsukuba, JP), and RIKEN (Tokyo, JP) will connect additional institutes sensibly enlarging the ensemble of ground clocks contributing to ACES.

The ground clocks connected to the ACES network are based on different atoms and ions, with transitions both in the microwave and in the optical domain. Microwave fountain clocks are today mature instruments, with fractional frequency stability and accuracy of a few parts in 10^{-16}, able to run on a very high duty cycle ($> 95\%$) [4,3]. They will be compared over the whole mission duration with the ACES clocks. Following the advances in optical frequency measurements using frequency combs, clocks based on the optical transitions of atoms and ions have made spectacular progress in the last years. Several optical clocks have demonstrated a stability of $3 \cdot 10^{-16}$ at 1 s, down to $2 \cdot 10^{-18}$ after 20000 s, and an accuracy in the 10^{-18} range [5,6,7,8,9,10]. These clocks are not yet as reliable as microwave fountain clocks, but with ACES they will be compared over intercontinental distances at 10^{-17} frequency resolution during dedicated measurement campaigns.

ACES is scheduled for launch with Space X in the first half of 2017. The ISS has a nearly circular orbit around the Earth with a mean elevation of 400 km, an orbital period of 5400 s, and an inclination of 51.6°. The first 6 months of operations will be devoted to the characterization and performance evaluation of the ACES clocks and links. In microgravity, it will be possible to optimize the interaction time of cesium atoms in the PHARAO clock and tune the linewidth of the atomic resonance by two orders of magnitude. After the clocks optimization, performance in the 10^{16} range both in frequency stability and accuracy are expected. In parallel, the ACES metrology links will be calibrated and characterized. During the second part of the mission (12 months, possibly extended to 30 months), the ACES clocks will be routinely compared to ground clocks operating both in the microwave and in the optical domain.

2 Scientific Objectives

2.1 Testing General Relativity with ACES

According to Einstein's theory of general relativity, identical clocks placed in different gravitational fields experience a frequency shift that depends on the difference between the Newtonian potentials at the clock positions. The comparison between the ACES clocks and ground-based atomic clocks will measure the frequency variation due to the gravitational redshift with a 35-fold improvement on the GP-A experiment [11], testing Einsteins prediction at the 2 ppm uncertainty level.

Time variations of fundamental constants can be measured by comparing clocks based on different atomic species and transitions [12,13]. Indeed, the energy of an atomic transition can be expressed in terms of the fine structure constant α and the two dimensionless constants m_q/Λ_{QCD} and m_e/Λ_{QCD}, depending on the quark mass m_q, the electron mass m_e, and the QCD mass scale Λ_{QCD} [14,15]. ACES will perform crossed comparisons of ground clocks both in the microwave and in the optical domain with a frequency resolution of $1 \cdot 10^{-17}$ in a few days of integration time. These comparisons will impose strong and unambiguous constraints on the time variations of the three fundamental constants reaching an uncertainty of $1 \cdot 10^{-17}$/yr after one year, down to $3 \cdot 10^{-18}$/yr after three years.

The foundations of special relativity lie on the hypothesis of Local Lorentz Invariance (LLI). According to this principle, the outcome of any local test experiment is independent of the velocity of the freely falling apparatus. In 1997, LLI tests based on the measurement of the round-trip speed of light have been performed by comparing clocks onboard GPS satellites to ground hydrogen masers [16]. In such experiments, LLI violations would appear as variations of the speed of light c

with the line-of-sight direction and the relative velocity of the clocks. ACES will perform a similar experiment by measuring relative variations of the speed of light at the 10^{-10} uncertainty level.

2.2 Applications

ACES will also demonstrate a new technique to map the Earth gravitational potential. It relies on a precision measurement of the Einstein's gravitational redshift between two clocks to determine the corresponding difference in the local gravitational potentials. The possibility of performing comparisons of ground clocks to the 10^{-17} frequency uncertainty level will allow ACES to resolve geopotential differences down to 10 cm on the geoid height.

A dedicated GNSS receiver onboard the ACES payload will ensure orbit determination of the space clocks. The receiver will be connected to the ACES clock signal, opening the possibility of using the GNSS network for space-to-ground clock comparisons.

The simultaneous operation of MWL and ELT will allow to cross calibrate the two links. Optical versus dual-frequency microwave measurements will provide useful data for the study of atmospheric propagation delays and for the construction of atmosphere mapping functions in S-band, Ku-band, and at optical frequencies. The ACES links will also deliver absolute ranging measurements, both in the microwave and in the optical domain.

3 ACES Status

The development status of the ACES clocks and links is discussed in the following.

3.1 PHARAO

PHARAO is a primary frequency standard based on laser cooled cesium atoms developed by LNE-SYRTE, LKB, and CNES. Its concept is very similar to ground-based atomic fountains. Atoms, launched in free flight along the PHARAO tube, cross a resonant cavity composed of two spatially separated interrogation zones where they interact with a microwave field tuned on the transition between the two hyperfine levels of the cesium ground state (9.192631770 GHz, from the SI definition of the second). In microgravity, the velocity of the atoms is constant and it can be continuously changed over almost two orders of magnitude (5 to 500cm/s), allowing the detection of atomic signals down to sub-Hz linewidth.

All PHARAO subsystems have passed the qualification tests: random vibration level of 10 g_{rms} and 30 g at 30Hz; storage temperature from -32 °C to +40 °C and operating temperature from +10 °C to +33 °C. Figure 3 shows the PHARAO flight model assembled on the ACES baseplate at CNES premises in Toulouse. During ground tests, PHARAO is operated under vacuum with the cesium tube aligned vertically and the atoms launched upwards at a velocity of 3.56 m/s. The space environment is emulated by changing the temperature at the clock baseplate and the magnetic field via large external Helmholtz coils. The clock performance tests lasted 4 months and ended in summer 2014. The capture, cooling, launch, and detection of cold atoms have been optimized. The frequency stability and the largest systematic frequency shifts of the clock have been measured. A short summary of the main results is given below.

$5 \cdot 10^8$ atoms are typically collected in the PHARAO optical molasses for a laser power of 13 mW/beam and a loading time of 1.5 s. During ground operation, this number is reduced to about $5 \cdot 10^7$ (laser power 5 mW per beam, loading time 200ms) to avoid saturation of the detection signal. The PHARAO Ramsey fringes are in full agreement with numerical simulations. The central fringe has a linewidth of 5.6 Hz corresponding to an interaction time of 90 ms. In microgravity, the linewidth can be reduced to 0.12 Hz at a launch velocity of 50 mm/s.

The PHARAO frequency stability (see Figure 4) has been measured as a function of the integration time τ by comparing the clock to the SYRTE mobile fountain FOM [17]. PHARAO Allan deviation is $3.15 \cdot 10^{-13}/\sqrt{\tau}$, while FOM is contributing with $1.3 \cdot 10^{-13}/\sqrt{\tau}$. The clock model predicts a frequency stability of $1.1 \cdot 10^{-13}/\sqrt{\tau}$ in microgravity. PHARAO and FOM frequencies agree to better than $2 \cdot 10^{-15}$.

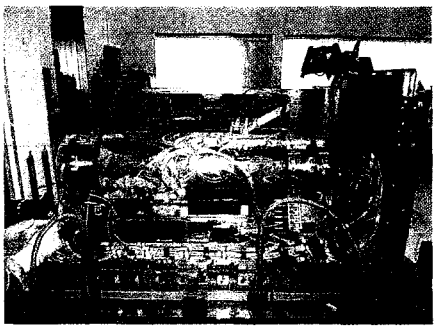

Figure 3 – The flight model of the PHARAO clock integrated on the ACES baseplate.

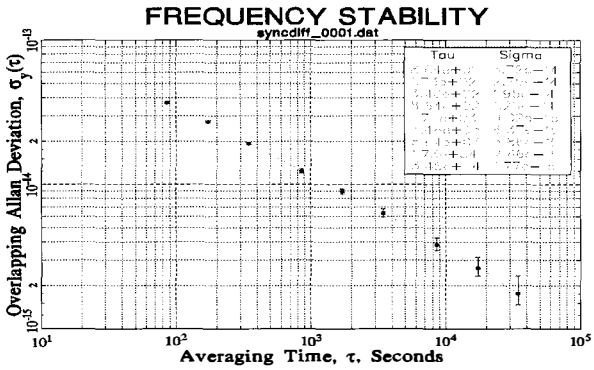

Figure 4 – PHARAO frequency stability on the ground measured against the mobile fountain clock FOM.

The frequency accuracy of the PHARAO clock has been analyzed and systematic frequency shifts are summarized in Table 1. The dominant frequency shift results from the second-order Zeeman effect. The high-contrast Ramsey profile obtained on the transition between m=1 Zeeman sub-levels corresponds to a magnetic field homogeneity better than $\delta B/B \sim 10^{-3}$ (B=1 mG) along the atomic trajectories. The orbital variations of the Earth magnetic field ($\pm 40\,\mu$T) remain an important issue as the overall attenuations factor of 270000 provided by the PHARAO μ-metal shields and the active compensation is not sufficient to control the corresponding frequency variations ($2 \cdot 10^{-16}$). Therefore, the magnetic field experienced by the atoms is periodically measured at a rate of 2 mHz by using the high sensitivity of the m=1 hyperfine resonance. The measurement lasts 10 seconds and has negligible influence on the overall clock stability. In this way, an uncertainty at the 10^{-17} level can be reched. The second main systematic effect is the black-body radiation shift [18]. The thermal behaviour of the cesium tube has been modeled using finite element analysis and its accuracy has been verified during thermal balance tests by using calibrated platinum resistors. The error on the temperature seen by the atomic ensemble is estimated to 56 mK, corresponding to a $1.5 \cdot 10^{-17}$ contribution of the black-body radiation shift to the clock accuracy. The cold collisions shift depends on the relative energy of colliding atoms and on the local density. The effect is measured by operating the clock with different atom numbers and densities and extrapolating the frequency shift to the zero-density limit. The number of atoms is varied by changing the frequency of the preparation cavity with optimized power to ensure that atomic densities are proportional to the atom numbers to better than 1%. On ground, the uncertainty is mainly limited by the measurement duration. In space, with typical velocities of 300 mm/s, a frequency shift of $1.5 \cdot 10^{-15}$ is expected. Measurements will be performed during

Table 1: Main systematic frequency shifts and uncertainties of PHARAO tested on ground.

Effect	Correction (10^{-15})	Uncertainty (10^{-16})
Magnetic field	181	< 1
Black-body shift	-17.6	< 1
Collisions	-7	12
Longitudinal phase gradient	3	6
Microwave recoil/lensing	0.12	< 1
Phase transients	< 1	< 1
Total	160.55	14

the whole mission duration to reach an uncertainty of $5 \cdot 10^{-17}$. The residual Doppler effect resulting from the inhomogeneous phase distribution of the microwave field inside the cavity has been calculated by numerical simulations and verified by measurements. On the ground, the longitudinal phase gradient is amplified by the atomic deceleration between the first and the second Ramsey interaction regions, producing a frequency shift of $3 \cdot 10^{-15}$. In space, a frequency shift of $3 \cdot 10^{-17}$ is expected for typical operating conditions. This effect is linear with the atomic velocity, but it remains coupled to the collisional shift. By varying both the launch velocity and the density over two orders of magnitude, we expect to reach an uncertainty of $5 \cdot 10^{-17}$ for the combined contribution. The effect of the transverse phase gradient in the cavity has been evaluated in collaboration with K. Gibble [3,4], who is also estimating the recoil shift produced by microwave photons (microwave lensing)[19]. The frequency shift is of the order of $1 \cdot 10^{-16}$ and it depends on the size of the atomic wave function and on the geometry of the cesium tube. In summary, the PHARAO clock is expected to have an accuracy of $1 - 3 \cdot 10^{-16}$ when operated in microgravity.

PHARAO is now in the ACES integration room at ADS premises in Friedrichshafen.

3.2 SHM

SHM is an active H-maser operating on the hyperfine transition of atomic hydrogen at 1.420405751 GHz. Developed by SpectraTime, SHM provides ACES with a stable fly-wheel oscillator. SHM is designed to fit into a volume of $390 \times 390 \times 590$ mm^3 and a mass of 42 kg, while still providing the frequency stability performance of a ground maser. To this purpose, the number of thermal shields has been reduced and a dedicated Automatic Cavity Tuning (ACT) system has been implemented to steer the resonance frequency of the maser cavity against thermal drifts. SHM ACT injects two tones, symmetrically placed around the H-maser signal. The two tones are coherently detected and the unbalance between their power levels is used to close a feedback loop acting on the cavity varactor and stabilizing the resonance frequency of the microwave cavity against temperature variations. This method allows SHM to reach fractional frequency stabilities down to $1.5 \cdot 10^{-15}$ at 10^4 s of integration time. Figure 5 shown the Allan deviation of the clock measured under stable laboratory conditions against a ground H-maser.

The SHM sensitivity to temperature and magnetic field variations has been measured. The thermal sensitivity can be counteracted by a fast servo of the ACES baseplate temperature ($< 600\,s$ time constant) and by the natural filtering of frequency fluctuations introduced by the thermal inertia of the instrument. In addition, SHM frequency variations can be calibrated as a function of temperature. SHM sensitivity to magnetic fields has been measured to about $8 \cdot 10^{-14}$/G. At this level, the magnetic field variations along the ISS orbit (± 0.4 G) are expected to introduce a degradation to the H-maser stability of $1 - 2 \cdot 10^{-14}$. These frequency fluctuations will be corrected by the ACES servo loops. In addition, magnetic field perturbations are suppressed to high degree when taking the difference over 100 s time intervals, as needed for the PHARAO accuracy evaluation. Tests will be performed to better characterize the H-maser sensitivity to external B-fields.

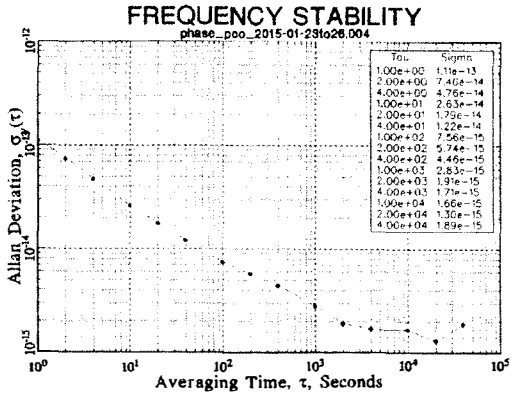

Figure 5 – SHM frequency stability measured against a ground H-maser.

The SHM flight model is under completion. Its delivery for integration in the ACES baseplate is expected in the first months of 2016.

3.3 MWL

The ACES microwave link is developed by ADS, TIMETECH, TZR, and EREMS. The proposed MWL concept is an upgraded version of the Vessot two-way technique used for the GP-A experiment in 1976 [11] and the PRARE geodesy instrument. The system operates continuously with a carrier frequency in the Ku-band. The high carrier frequencies of the up and down links (13.5 GHz and 14.7 GHz respectively) allow for a noticeable reduction of the ionospheric delay. A third frequency in the S-band (2.2 GHz) is used to determine the Total Electron Content (TEC) and correct for the ionospheric time delay. A PN-code modulation (100 Mchip/s) on the carrier removes the phase ambiguity between successive comparison sessions separated by large dead times. The system is designed for multiple access capability, allowing up to 4 simultaneous ground users distinguished by the different PN-codes and Doppler shifts.

The engineering model of the flight segment electronic unit has been completed and tested in end-to-end configuration with the ground terminal electronics in the presence of signal dynamics (attenuation and Doppler frequency variations as predicted along the ISS orbit). MWL long-term stability is ensured by the continuous calibration of the receiver channels provided by a built-in test-loop translator. For shorter durations (<300 s), the time stability is driven by the noise performance of the Ku-band transmitter and receiver and the DLL (Delay-Locked Loop) boards. The 100 MHz chip rate allows to reach a time stability at the 5 ps level already with code measurements. However, the ultimate performance is achieved with the carrier phase measurements, whose time stability is at the level 200 fs at about 100 s of integration time in the presence of signal dynamics. The thermal sensitivity of the system has been calibrated. The sensitivity to a series of key parameters such as clock input power, received signal-to-noise density ratios, supply voltage, Doppler, and Doppler rate has also been measured.

MWL ground terminal (GT) electronics are similar to the MWL flight hardware, symmetry being important in a two-way system to reduce instrumental errors. The electronic unit of the MWL GT has been rigidly attached to the antenna unit to reduce phase instabilities due to the tracking motion. The Ku-band signal is delivered to the antenna feeder via a waveguide; a high stability RF cable is used for the S-band. The antenna is a 60 cm offset reflector with a dual-band feed system automatically pointed in azimuth and elevation by a steering mechanism. A computer controls the steering unit based on ISS orbit prediction files, collects telemetry and science data both from the local clocks and the MWL GT electronics, and it interfaces directly with the ACES Users Support and Operation Center (USOC). The system is housed below a protective radome

cover, which also allows to stabilize the temperature of the enclosed volume by an air conditioning system, part of a separate service pallet. The thermal design allows to operate the MWL GT for an external temperature between −30°C and +45°C.

The MWL flight model is under assembly and board level tests have already started. The delivery of MWL flight segment electronics for integration in the ACES payload is expected by end 2015. The deployment of the ACES MWL ground terminals will start in the fall of 2015.

3.4 ELT

ELT, acronym for European Laser Timing, is an optical link based on picosecond laser pulses exchanged between Satellite Laser Ranging (SLR) stations on ground and the ACES payload. The onboard hardware consists of a corner cube reflector, a Single-Photon Avalanche Diode (SPAD), and an event timer board connected to the ACES time scale. Laser pulses fired towards the ISS are detected by the SPAD diode and stamped in the ACES scale. At the same time, the ELT reflector re-directs the laser pulses towards the ground station. The measurement of the start and return times on ground and of the detection time in space is then used to determine the desynchronization between space and ground clocks as well as the range.

Developed by the Technical University of Prague and CSRC, the SPAD diode has been tested in conjunction with a laboratory time tagging board providing sub-picosecond resolution. The time deviation of the combined system has a floor slightly below 200 fs. Peak-to-peak time fluctuations amount to a few picoseconds over several days of measurement. The detector is extremely robust against stray light and temperature variations. The temperature sensitivity has been measured between −60°C and +70°C showing a mean slope as low as 0.48 ps/K.

The flight model of the detector is expected to be delivered after this summer. The corner cube reflector is already integrated.

Acknowledgments

The development of the ACES mission is a collective effort and the authors would like to thank all participants, in particular the ACES Investigators Working Group (IWG), the ACES project team at ESA and ADS, the PHARAO team at CNES, SYRTE, LKB, TAS, Sodern, Erems, CS, the SHM team at SpectraTime, the University of Prague team, the Technical University of Münich team, and the data analysis team at SYRTE for their contributions. This work is supported by ESA, CNES, and CNRS.

References

1. C. Salomon *et al*, C. R. Acad. Sci. Paris **t.2 Séries 4**, 1313 (2001).
2. L. Cacciapuoti and C. Salomon, Eur. Phys. J. Special topics **172**, 57 (2009).
3. R. Li *et al*, Metrologia **48**, 283 (2011).
4. J. Guéna *et al*, Phys. Rev. Lett **106**, 130801 (2011).
5. T. Rosenband *et al*, Science **319**, 1808 (2008).
6. A.D. Ludlow *et al*, Science **319**, 1805 (2008).
7. N. Hinkley *et al*, Science **341**, 1215 (2013).
8. B.J. Bloom *et al*, Nature **506**, 71 (2014).
9. I. Ushijima *et al*, Nature Photonics **9**, 185 (2015).
10. T.L. Nicholson *et al*, Nature **6**, 6896 (2015).
11. R.F.C. Vessot *et al*, Phys. Rev. Lett. **45**, 2081 (1980).
12. N. Huntermann *et al*, Phys. Rev. Lett. **113**, 210802 (2014).
13. R.M. Godun *et al*, Phys. Rev. Lett. **113**, 210801 (2014).
14. V.V. Flambaum *et al*, Phys. Rev. D **69**, 115006 (2004).
15. V.V. Flambaum *et al*, Phys. Rev. C **73**, 055501 (2006).
16. P. Wolf and G. Petit, Phys. Rev. A **56**, 4405 (199).
17. J. Guéna *et al*, IEEE Trans. Ultrason. Ferroelec. Freq. Contr. **59**, 391 (2012).
18. W. Itano *et al*, Phys Rev. A **25**, 1233 (1981).
19. K. Gibble, Phys. Rev. A **90**, 015601 (2014).